



NASATM-58222

# NASA Technical Memorandum 58222

NASA-TM-58222 19800006753

## Preliminary Results of Penetrator Field Test Program—Tonopah, Nevada, April 16-28, 1979

FOR REFERENCE

Maxwell B. Blanchard, Uel Clanton, Mischelle Dalbey, Victor Rhoder, and James P. Murphy

NOT TO BE TAKEN FROM THIS ROOM

October 1979

LIBRARY COPY

MAR 21 1980

LANGLEY RESEARCH CENTER  
LIBRARY, NASA  
HAMPTON, VIRGINIA



National Aeronautics and Space Administration

Lyndon B. Johnson Space Center  
Houston, Texas 77058

1998

1999

2000

2001

2002

2003

2004

2005

2006

2007

2008

2009

2010

2011

2012

2013

2014

2015

2016

2017

2018

2019

2020

2021

2022

2023

2024

2025

2026

2027

2028

2029

2030

2031

2032

2033

LaRC: ITS/Technical Library  
National Aeronautics and  
Space Administration  
Ames Research Center  
Moffett Field, California 94035



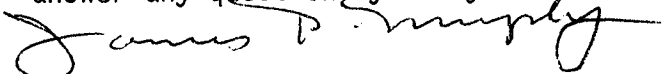
Reply to Attn of: **SPT:244-7/213**

**TO: DISTRIBUTION**

**FROM: SPT/James P. Murphy, Assistant Chief  
Project Technology Branch**

**SUBJECT: Penetrator Survivability Tests**

A number of activities were undertaken by Ames in FY78 with a goal of further developing the Penetrator and answering questions in key scientific and technical areas. These activities included a series of Survivability Tests conducted by Ames, the Johnson Space Center (JSC), and Sandia. The Survivability Tests have been successfully completed, and the results are quite interesting. I have enclosed a copy of the report (NASA TM 58222) describing these test results for your information. A more comprehensive description of all the Penetrator activities and results through 1979 will be prepared in the near future for distribution in the form of a NASA TM. Max Blanchard at JSC (713-483-3274) or I (415-965-6520) will be happy to answer any questions you may have.



James P. Murphy

**Enclosure:  
NASA TM 58222**



NASA Technical Memorandum 58222

Preliminary Results of Penetrator Field  
Test Program—Tonopah, Nevada,  
April 16-28, 1979

Maxwell B. Blanchard, Uel Clanton, and Victor Rhoder  
*Lyndon B. Johnson Space Center*  
*Houston, Texas*

Mischelle Dalbey  
*Lunar and Planetary Institute*  
*Houston, Texas*

James P. Murphy  
*Ames Research Center*  
*Moffett Field, California*

**NASA**

National Aeronautics and  
Space Administration

**Scientific and Technical  
Information Office**

1979

N80-15012 #



## CONTENTS

Section	Page
SUMMARY . . . . .	1
INTRODUCTION . . . . .	1
PROCEDURE . . . . .	2
RESULTS AND DISCUSSION . . . . .	4
CONCLUSIONS . . . . .	6
REFERENCES . . . . .	8

TABLES

Table		Page
I	PRETEST CONDITIONS . . . . .	9
II	POST-TEST CONDITIONS . . . . .	10
III	LOCATION OF SCRAPE MARKS ON PENETRATOR AFTER CLEARING CATCHER BLOCK BUT BEFORE IMPACTING TARGET . . . . .	11
IV	STATUS OF HIGH-SPEED MOTION PICTURE FILM . . . . .	12



## FIGURES

Figure		Page
1	Mars penetrator (0.63 scale) configuration fired in tests at Tonopah, Nevada, in April 1979 . . . . .	13
2	Layout of test site. The penetrator impact points are located at one-half the radius of the rock. Test numbers are shown beneath each target arrangement . . . . .	14
3	Sabot used to adapt penetrator to 7.6-centimeter (3 inch) air gun . . . . .	15
4	Penetrator and sabot assembled and mounted in breech of air gun . . . . .	16
5	Air gun shown in vertical position (orientation from which measurements were made) and grid frame located beneath trailer before test 6. Camera pallets are located on the ground near the front and rear of the trailer . . . . .	17
6	Penetrator being fired by air gun (test 6). The blast of air which replaces the penetrator produces the cloud of dust obscuring the grid and the target . . . . .	17
7	Grid network that provided a three-dimensional frame of reference for the high-speed motion pictures. The grid consisted of 1.3-centimeter (0.5 inch) aluminum bars welded together at 15.2-centimeter (6 inch) intervals. The grid was staked to the ground to prevent movement during the tests, but airblast-produced vibration occasionally blurred the image of the grid in the films . . . . .	18
8	Layout of motion picture cameras, grid frame, and penetrator impact point . . . . .	19
9	Cratered area after penetrator passed through the 13-centimeter (5 inch) diameter rock shown in figure 7. The penetrator stopped approximately 4 meters (12 feet) beneath the surface after impact. Several broken fragments of the original rock are near the grid . . . . .	20
10	A 1.2-meter (4 foot) diameter hole was drilled with a bucket auger adjacent to the hole made by the penetrator . . . . .	21
11	One side of the hole was removed to expose a complete cross section of the hole made by the penetrator . . . . .	22

12 Cross section of the hole made by the penetrator in test 2. The distance from the surface of the ground to the nose of the penetrator is 323 centimeters (127 inches). The penetrator had a final orientation of 89°20' from the horizontal along a bearing of 60°. A change in direction occurred just after the penetrator passed through the 5-centimeter (2 inch) diameter rocks . . . . . 23

13 Cross sections of the hole after each penetrator test

(a) Tests 1 to 3 . . . . . 24

(b) Tests 4 to 6 . . . . . 25

(c) Tests 7 to 9 . . . . . 26

(d) Tests 10 to 12 . . . . . 27

(e) Test 13 . . . . . 28

14 A cyclographic projection showing penetrator orientations for each test. Three points were plotted for tests 5, 6, 7, 10, 11, 12, and 13: orientation in the air gun (data from table I), orientation during free flight (data from high-speed motion pictures), and final orientation (data from table II). Two points were plotted for all other tests: orientation in the air gun and final orientation. The bearing for each point is read on the outside perimeter as a compass direction. The dip angle is read along a radius from the origin to either E or W using the graduated 10° increments from 0° to 90°. The procedure used to locate these points is described in reference 6 . . . . . 29

## SUMMARY

A series of 13 tests of 0.63-scale solid steel penetrators fired by an air gun was performed to determine the deflection caused by impact with various sizes of volcanic rocks resting on or buried within compacted sediments. All penetrators used were identical in size, shape, weight, impact velocity, and general orientation. The targets were prepared using a basalt from the Malpais lava flow in New Mexico. This basalt, a tholeiite having a porosity of 20 to 30 percent, was selected because of its similarity to Martian volcanic rock.

Photographic coverage of the tests consisted of two types of high-speed motion and 70-millimeter still photography. Two cameras, each having a film speed of approximately 10 000 frames/sec, were used to obtain closeup views of the penetrator. Timing marks were exposed on the film to assist photo-interpretation. The final orientation of all penetrators was measured in situ by means of a large access hole drilled adjacent to the point of impact.

The results of the tests suggest that no catastrophic penetrator failure is likely to occur and that major deflections are caused only by rocks  $\geq 10$  times the diameter of the impacting body.

## INTRODUCTION

The purpose of these field tests was to determine the deflection caused to subscale (0.63 scale) penetrators impacting volcanic rocks of various sizes resting on top of, and within, compacted sediments. During the tests, all penetrators were identical in size, shape, weight, impact velocity, and general orientation. For these tests, the final orientation of the buried penetrators is assumed to be primarily a consequence of the size, the shape, and the depth of the rocks encountered during impact, although some variation in impact angle was documented. Previously, a theoretical study examined the capability of a penetrator to survive impact on Mars (ref. 1). On the assumption that the hazardous size range of rocks was 0.2 to 5 times the diameter of the penetrator, it was found that the probability of catastrophic penetrator failure was 10 percent. The field tests do not confirm that the size range used in the theoretical study will cause a catastrophic penetrator failure. These tests indicate that no failure is likely to occur. Major penetrator deflections are only caused by rocks 10 times and greater in diameter than the impacting body, and then deflection is highly dependent upon the fracture planes that develop in the rock as it breaks apart.

The authors are greatly indebted to L. Polaski, NASA Ames Research Center, for his assistance during the tests and the preparation of this report. We sincerely appreciate the support and guidance given to us by A. Foster,

C. Dalton, W. Jacobi, and C. Wilson, Sandia Laboratory, while preparing for and conducting the tests at the Tonopah Test Site, Nevada.

In compliance with the NASA's publication policy, the original units of measure have been converted to the equivalent value in the Système International d'Unités (SI). As an aid to the reader, the SI units are written first and the original units are written parenthetically thereafter. Field measurements, which were performed to within  $\pm 1/4$  inch, are converted to the nearest centimeter.

## PROCEDURE

Thirteen scaled penetrators were fired into prepared targets at the Sandia Tonopah Test Range, Nevada, during April 16 to 28, 1979. The firings were conducted with 0.63-scale,<sup>1</sup> solid penetrators (steel alloy 4340). The penetrators were 62.86 centimeters (24.75 inches) long and 5.71 centimeters (2.25 inches) in diameter and were painted white with 0.63-centimeter (0.25 inch) wide black stripes every 7.6 centimeters (3 inches) along the body (fig. 1). The targets consisted of three different arrangements of rocks buried beneath or lying on the homogeneous compacted dry playa sediments (fig. 2). The first series of tests consisted of penetrator impacts into layers of rocks (15-centimeter (6 inch) thick layers of 2- and 5-centimeter (3/4 and 2 inch) diameter rocks and single layers of 13-, 18-, and 61-centimeter (5, 7, and 24 inch) diameter rocks) buried 30 centimeters (12 inches) below the playa surface. The second series of tests consisted of penetrator impacts into single rocks (5, 13, 18, and 61 centimeters (2, 5, 7, and 24 inches) in diameter) lying on the playa surface. The third series of tests consisted of penetrator impacts into layers of rocks (a 15-centimeter (6 inch) thick layer of 5-centimeter (2 inch) diameter rocks and single layers of 13- and 18-centimeter (5 and 7 inch) diameter rocks) lying on the playa surface. In each test, the penetrator was aligned to strike a target rock that had been selected by boresighting the gun at a half-radius point.

The rock selected for this test was a basalt from the Malpais lava flow near Tularosa, New Mexico, that had been removed by jackhammer, then crushed and sized. This basalt, a tholeiite having a porosity of 20 to 30 percent, was selected because of its similarity to Martian volcanic rocks (ref. 2). The type of flow varies from pahoehoe to aa. Before this basalt was selected, field tests were conducted in the Malpais with 0.63-scale penetrators (ref. 3). The depth of penetration was about 61 centimeters (24 inches) during these tests; thus, the volcanic rock had an S number of less than 1 (about 0.7) in accordance with Young's penetration equations (ref. 4), which verified similarity with previous tests in terrestrial analogs of Martian volcanic rocks.

The 7.6-centimeter (3 inch) diameter air gun used to fire these penetrators was operated by Sandia staff from Albuquerque, New Mexico. Because the

---

<sup>1</sup>Scaled to Mars penetrator configuration based on diameter, where the ratio of weight to cross-sectional area  $W/A$  is kept constant.

inside diameter (7.818 centimeters (3.078 inches)) of this air gun was too large for the 0.63-scale penetrator (5.71 centimeters (2.25 inches) diameter), an aluminum sabot was used to guide the projectile down the gun barrel (fig. 3). The aft end of the penetrator was mounted in the sabot and held with three setscrews. The sabot and the penetrator were mounted in the breech (fig. 4), where another setscrew was used to hold the sabot-penetrator assembly and prevent it from falling out when the gun was erected to the vertical position. However, on one test, the penetrator fell as the gun was erected and broke the target rock. The target was rebuilt using another rock before firing the shot (test 4). Although the sabot was stripped from the penetrator by a wood block, on six tests, the sabot went through the block and impacted the ground about 150 milliseconds after the penetrator disappeared from the field of view.

The orientation of the air-gun barrel after being erected (fig. 5) was measured in two directions along the same axis as the grid frame staked to the ground as a basis of reference for photography. The orientation of the air gun was within  $\pm 0^{\circ}40'$  of vertical for all tests (table I). The air-gun tank pressure at firing was  $10\,997\text{ kN/m}^2$  ( $1595\text{ lb/in}^2$ ), which produced an impact velocity of  $150\text{ m/sec}$  ( $492\text{ ft/sec}$ ) for the penetrator (fig. 6).

An L-shaped metal frame painted orange, having 1.3-centimeter (0.5 inch) bars welded in a grid pattern on 15.2-centimeter (6 inch) intervals (fig. 7), was used as a reference for tracking penetrator movement. This grid was leveled using a Brunton compass for tests 4 to 13; the orientation of the grid is not precisely known for tests 1 to 3.

Photographic coverage of the tests consisted of two types of high-speed motion and 70-millimeter still photography. The high-speed motion pictures were taken of all tests except when the film broke or the camera jammed.<sup>2</sup> Two Milliken cameras, having a film speed of about 400 frames/sec, were used to obtain overall views of the air gun, of the penetrator impact event, and of debris flying from the impact. One Hycam and one Fastax camera, each having a film speed of about 10 000 frames/sec, were used to obtain closeup views of the penetrator. These cameras were positioned perpendicular to the grid frame (fig. 8) to enable reconstructing a three-dimensional orientation for the penetrators during flight and impact. Other uses of these high-speed motion pictures include measuring impact velocity, deceleration, and lateral displacements and documenting rock failure during impact. Timing marks were exposed on the films to assist photointerpretation. Although a timing signal of 10 000 hertz was attempted on all high-speed photography, only 100- and 1000-hertz signals occurred on six films and six films had only an incomplete interranger instrumentation group (IRIG) format A signal or none at all. The lack of reliable short-period timing signals seriously limits the photointerpretation activity. Still photograph (70 millimeter) coverage of the cratered area after impact (fig. 9) was taken in stereo; down-hole photography was obtained of each test to enable making a photomosaic of the entire hole along its longitudinal axis.

---

<sup>2</sup>No film was obtained from one of the two Milliken cameras on tests 4 and 6 and from the Hycam camera on tests 8 and 9.

A drill rig with a large bucket auger (fig. 10) was used to drill a 1.2-meter (4 foot) diameter hole adjacent to the point of impact (fig. 11); by this means, a cross section could be made of the entire length of the hole (fig. 12). The final orientation of all penetrators was measured in situ.

## RESULTS AND DISCUSSION

The pretest conditions listed in table I include the test number, the rock size, the target arrangement, and the orientation of the air gun, the sabot catcher block, and the grid frame. The post-test conditions listed in table II include the orientation of the penetrator at different depths as it passed through the ground to its final location, the lateral displacement of the penetrator nose from its point of impact to its final resting place, the distance material was thrown away from the point of impact, and the status of the sabot.

The general trend indicates that the larger rocks produced greater angles of deflection for impacting penetrators. For layers of buried rocks (tests 1 to 5), the 2-centimeter ( $3/4$  inch) diameter rocks induced about the same deflection as the 13-centimeter (5 inch) diameter rocks. However, the 18- and 61-centimeter (7 and 24 inch) diameter rocks produced progressively greater angles of deflection,  $10^{\circ}$  and  $11^{\circ}30'$ , respectively. A noteworthy feature of test 5 is that the penetrator apparently passed through an angle of deflection of  $26^{\circ}$  about 61 centimeters (24 inches) beneath the surface as it followed the fracture plane produced when the rock broke apart, yet its final orientation about 190 centimeters (75 inches) deep showed a much smaller angle of deflection ( $11^{\circ}30'$ ). For layers of surface rocks (tests 9, 10, and 12), only small angles of deflection were observed. Test 10 had the greatest angle,  $2^{\circ}30'$ . For single rocks at the surface (tests 6 to 8, 11, and 13), the angle of deflection increased gradually as the rock diameter increased. For the 5-, 13-, and 18-centimeter (2, 5, and 7 inch) diameter rocks, the angles of deflection were  $2^{\circ}00'$ ,  $9^{\circ}00'$ , and  $8^{\circ}20'$ . The greatest angles of deflection were observed when the penetrator impacted rocks with a diameter of 61 centimeters (24 inches). The angles of deflection were  $19^{\circ}00'$  and  $56^{\circ}10'$ . In shot 11, the penetrator passed through a large angle of deflection ( $60^{\circ}$ ) about 38 centimeters (15 inches) beneath the surface as it followed the fracture plane where the rock broke apart. Again, the penetrator's path straightened as it continued to travel, and its final angle of deflection was only  $19^{\circ}$ . It was not possible to measure the maximum angle of deflection by reconstructing the rock in shot 13 because the target moved as the penetrator was uncovered.

The size of rock necessary to prevent breakage when the penetrator passes through or is captured is a question that should be studied. Previous tests in basalt at Amboy Crater, California (ref. 5), and Tularosa, New Mexico (ref. 3), did not produce angles of inclination larger than a few degrees. In these tests, the penetrator was captured in the basalt and the rock did not break apart.

A cross section of the path of each penetrator through the ground is shown in figure 13. To compare the orientation of the penetrator in the air

gun before firing with its orientation during free flight and in the ground after the test, the data from tables I and II and from the high-speed motion pictures have been plotted on a cyclographic projection (fig. 14). The orientation of the penetrators in the gun and in the ground has been plotted on the figure for all tests. However, free-flight orientation of the penetrators is shown for only 7 (tests 5, 6, 7, 10, 11, 12, and 13) of the 13 tests. Data were not plotted for tests 1, 2, 3, and 4 because of poor image quality and for tests 8 and 9 because only a single film was obtained. Films from both cameras (Fastax and Hycam) are required to plot the true orientation of the penetrator during free flight. A single film provides only an apparent orientation.

If the orientations of the penetrator in the air gun, during free flight, and in the ground were identical, then the various symbols from a single test would plot in the same location (e.g., test 12). An evaluation of the orientations indicates that the gun and free-flight penetrator azimuths are within  $1^\circ$  for 4 (tests 5, 6, 12, and 13) of the 7 tests that can be evaluated. When the free-flight and in-ground penetrator orientations are compared, the azimuths are within  $45^\circ$  for 5 (tests 6, 7, 10, 12, and 13) of the 7 tests, and the dips are within  $10^\circ$  for 11 of the 13 tests.

The high-speed motion pictures show the penetrator usually impacted the surface at some small angle off vertical (probably a consequence of the sabot being stripped from the penetrator). The penetrator path appears to straighten and becomes more vertical as it enters the ground. Typically, an elliptical entry hole is produced that gradually becomes circular at a depth of about 45 centimeters (18 inches).

Although the tests are not conclusive, the data indicate that, for most tests, the final orientation of the penetrator in the ground is related to its free-flight orientation, so long as the impact is within  $4^\circ$  of vertical. This observation holds for impacts into rock sizes as great as 10 times the diameter of the penetrator.

The high-speed motion pictures show the penetrator entering the field of view of the camera at angles inclined to the vertical grid frame as high as  $5^\circ$ . The greatest angle the penetrator could have in the gun barrel, as long as the penetrator and sabot are together, is  $0.2^\circ$ . Even if the penetrator and sabot somehow separated inside the barrel, the angle could still not be greater than  $1.9^\circ$ . Consequently, the penetrator must be deflected after it leaves the muzzle. Although the evidence is circumstantial, the change in penetrator orientation during flight most probably occurs as the sabot is stripped from the penetrator by the wood block. Since this problem was not known during the tests because of poor quality or undeveloped film, the flight of the sabot-penetrator assembly leaving the muzzle before impacting the wood block was not photographed. The photography was taken only after the penetrator cleared the block. Because the seriousness of the problem was not recognized until after the tests were completed and all the film was developed, only casual information is available to document the problem.

After the first seven shots, in which the sabot passed through a single block six of seven times, two blocks were installed to stop the sabot. The dual-block arrangement was effective; the sabot stopped just short of full penetration of the first block. Typically, the top block had a pronounced asymmetrical bulge of shattered wood on its bottom surface after the shot. On the basis of two observations, the bottom block had black scrape marks oriented  $180^\circ$  apart along the interior walls of the center hole. High-speed photography from all tests except 2 and 9 show at least one scrape mark on one side of the penetrator. The center of the first scrape or scrapes typically occurs about 11 centimeters (4-1/4 inches) from the tip of the nose. A second and third series of scrapes occur on shots 10, 11, and 12 approximately 41 and 57 centimeters (16 and 22-1/2 inches) from the tip of the nose. The motion of the penetrator and/or block whereby paint can be selectively and somewhat consistently abraded remains unclear. Table III summarizes the position of the scrape marks.

It is uncertain whether photointerpretation of the high-speed motion pictures will solve the problems enumerated previously because the quality of the images is very poor for most tests. Most frequently, the black horizontal stripes on the penetrator cannot be seen without special processing, and even in the best films, the stripes are blurred and/or faint. Also, in some cases, the grid frame cannot be adequately referenced because it began vibrating from the airblast before the penetrator passed the grid. Unfortunately, the lack of 10 000-hertz timing marks on 12 of the 24 films causes a serious difficulty for any time-dependent measurements or calculations, and it may not be possible to overcome the loss of a time base. Table IV shows the current status of the high-speed motion pictures for the 13 tests (24 films). There are only four tests for which films from two different views  $90^\circ$  apart have the 10 000-hertz timing marks, and only two of these four tests have usable images.

Results of these tests must be evaluated with current information about the type and size of Martian surface rocks before any predictions can be made about penetrator survival on a Mars mission. Full-scale penetrators having the mission configuration and equipped with umbilicals and afterbodies should be considered for future testing and development studies. Full-scale tests would eliminate the uncertainties associated with scaling and modeling the effects of the impact.

## CONCLUSIONS

The following conclusions and recommendations are based on the penetrator field tests.

1. It appears that surface layers and buried layers of rocks which have diameters as large as about 3 times the penetrator diameter cause only small ( $<10^\circ$ ) angles of deflection of the penetrator during its passage. Typically, single rocks at the surface cause greater deflections, and, as the rock diameter increases, so does the final angle of deflection of the penetrator.



2. Only large single rocks (>10 times the penetrator diameter) caused deflections appreciably greater than  $10^{\circ}$ . Even then, during two tests (tests 5 and 11), the penetrator curiously showed a tendency to become more vertical as it continued its passage through the ground.

3. The large deflection angles followed by the penetrator are a consequence of the fracture planes that develop in the rock as it breaks apart. Just how large a rock must be before the penetrator passes through it (or stops in it) without the rock breaking apart is a question which needs to be addressed. Previous tests in basalt at Amboy Crater, California, and Tularosa, New Mexico, did not produce angles of inclination larger than a few degrees, and the penetrator did not pass through the basalt breaking the rock apart.

4. Results of these tests must be evaluated with current information about the type and size of Martian surface rocks before any predictions can be made about penetrator survival on a Mars mission.

5. Full-scale penetrators having the mission configuration and equipped with umbilicals and afterbodies should be considered for future testing and development studies. Full-scale tests would eliminate the uncertainties associated with scaling and modeling the effects of the impact.

Lyndon B. Johnson Space Center  
National Aeronautics and Space Administration  
Houston, Texas, September 20, 1979  
152-85-00-00-72

## REFERENCES

1. Manning, Larry A., ed.: Mars Surface Penetrator: System Description. NASA TM-73243, 1977.
2. Bunch, T. E.; Quaide, William L.; and Polkowski, George: Initial Basalt Target Site Selection Evaluation for the Mars Penetrator Drop Test. NASA TM X-73111, 1976.
3. Nakamura, Yosio; Latham, Gary V.; Frohlich, Cliff; Blanchard, Maxwell B.; and Murphy, James P.: Field Measurements of Penetrator Seismic Coupling in Sediments and Volcanic Rocks. NASA TM-78572, 1979.
4. Young, C. W.: Empirical Equations for Predicting Penetration Performance in Layered Earth Materials for Complex Penetrator Configurations. Rep. SC-DR-720523, Sandia Laboratories, 1972.
5. Blanchard, M.; Bunch, T.; Davis, A.; Shade, H.; Erlichman, J.; and Polkowski, G.: Results of Analyses Performed on Basalt Adjacent to Penetrators Emplaced Into Volcanic Rock at Amboy, California, April 1976. NASA TP-1026, 1977.
6. Bloss, F. Donald: An Introduction to the Methods of Optical Crystallography. Holt, Rinehart and Winston (New York), 1961, pp. 214-223.

TABLE I.- PRETEST CONDITIONS

Test no.	Rock diam, <sup>a</sup> cm (in.)		Rock arrangements	Trailer bearing	Orientation of grid frame		Orientation of air gun		Orientation of sabot catcher block	
					Bearing	Dip	Bearing	Dip	Bearing	Dip
1	2	(3/4)	Buried layer	E	SE	(b)	SE	90°00'	(b)	(b)
					SW	(b)	NE	89°31'	(b)	(b)
2	5	(2)	Buried layer	E	SE	(b)	SE	90°00'	(b)	(b)
					SW	(b)	SW	90°00'	(b)	(b)
3	13	(5)	Buried layer	E	SE	(b)	SE	90°00'	(b)	(b)
					SW	(b)	SW	89°50'	(b)	(b)
4	18	(7)	Buried layer	115°	150°	Vertical <sup>c</sup>	150°	90°00'	(b)	(b)
					240°	Vertical <sup>c</sup>	60°	89°40'	(b)	(b)
5	61	(24)	Buried layer	156°	190°	Vertical <sup>c</sup>	190°	90°00'	(b)	(b)
					280°	Vertical <sup>c</sup>	100°	89°30'	(b)	(b)
6	5	(2)	Single rock at surface	85°	125°	Vertical <sup>c</sup>	125°	90°00'	(b)	(b)
					215°	Vertical <sup>c</sup>	215°	90°00'	(b)	(b)
7	13	(5)	Single rock at surface	112°	145°	Vertical <sup>c</sup>	145°	90°00'	(b)	(b)
					235°	Vertical <sup>c</sup>	55°	89°30'	(b)	(b)
8	18	(7)	Single rock at surface	155°	180°	<sup>d</sup> 90°00'	180°	90°00'	(b)	(b)
					270°	<sup>d</sup> 90°00'	270°	89°30'	(b)	(b)
9	5	(2)	Layer on surface	28°	60°	<sup>d</sup> 90°00'	60°	90°00'	60°	0°40'
					150°	<sup>d</sup> 90°00'	150°	90°00'	330°	0°50'
10	13	(5)	Layer on surface	84°	123°	<sup>d</sup> 90°00'	123°	90°00'	123°	0°40'
					213°	<sup>d</sup> 90°00'	33°	89°50'	213°	0°40'
11	61	(24)	Single rock at surface	155°	197°	<sup>d</sup> 90°00'	197°	90°00'	17°	0°30'
					287°	<sup>d</sup> 90°00'	107°	89°50'	107°	0°20'
12	18	(7)	Layer on surface	28°	80°	<sup>d</sup> 90°00'	80°	90°00'	260°	0°10'
					170°	<sup>d</sup> 90°00'	350°	89°20'	350°	0°40'
13	61	(24)	Single rock at surface	115°	160°	<sup>d</sup> 90°00'	160°	90°00'	160°	0°10'
					250°	<sup>d</sup> 90°00'	250°	90°00'	70°	0°20'

<sup>a</sup>Measured to within ±1/4 inch.<sup>b</sup>Not available.<sup>c</sup>Measured to within ±1°.<sup>d</sup>Measured to within ±0°10'.

TABLE II.- POST-TEST CONDITIONS

Test no.	Orientation during penetration			Max lateral displacement of nose, <sup>a</sup> cm (in.)	Distance debris traveled from hole, <sup>a</sup> m (ft)	Sabot location
	Depth, <sup>a</sup> cm (in.)	Bearing	Dip			
1	157 (62)	305°	88°00'	(b)	(b)	Hole
	262 (103)	130°	87°20'			
	335 (132)	143°	86°20'			
2	122 (48)	210°	89°30'	30 (12)	(b)	Block
	236 (93)	285°	88°50'			
	323 (127-1/4)	60°	89°20'			
3	76 (30)	272°	87°10'	(b)	(b)	Hole
	203 (80)	295°	87°00'			
	328 (129-1/4)	320°	86°40'			
4	15 (6)	(b)	88°00'	47 (18-1/2)	(b)	Hole
	140 (55)	27°	82°00'			
	264 (104)	20°	80°00'			
	327 (128-3/4)	20°	80°00'			
5	61 (24)	160°	64°00'	61 (24)	(b)	Hole
	190 (74-3/4)	125°	78°30'			
6	96 (38)	77°	87°50'	9 (3-3/4)	28 (91)	Hole
	188 (74)	110°	88°20'			
	332 (130-3/4)	112°	88°00'			
7	341 (134-1/4)	45°	81°00'	53 (21)	43 (142)	Hole
8	39 (15-1/2)	152°	87°10'	29 (11-1/2)	34 (112)	Block
	69 (27)	140°	81°40'			
	327 (128-3/4)	140°	81°40'			
9	340 (133-3/4)	260°	89°20'	11 (4-1/2)	6 (20)	Block
	327 (128-3/4)	60°	87°30'			
10	327 (128-3/4)	60°	87°30'	16 (6-1/4)	>30 (>100)	Block
11	38 (15)	(b)	30°00'	51 (20)	7 (24)	Block
	213 (84)	310°	71°00'			
12	327 (128-3/4)	260°	89°40'	2 (1)	3 (11)	Block
13	119 (47)	150°	33°50'	98 (38-3/4)	30 (99)	Block

<sup>a</sup>Measured to within ±1/4 inch.<sup>b</sup>Not available.

TABLE III.- LOCATION OF SCRAPE MARKS<sup>a</sup> ON PENETRATOR AFTER  
CLEARING CATCHER BLOCK BUT BEFORE IMPACTING TARGET

Test no.	Approx. distance, <sup>b</sup> cm (in.), from tip of nose to center of scrape		Comments
	Hycam view	Fastax view	
1	?	11 (4-1/2)	Hycam image poor; penetrator may be scraped at 11 cm (4-1/2 in.)
2	No scrapes	No scrapes	Penetrator paint undamaged
3	15 (6)	15 (6)	Single scrape photographed by both cameras
4	11 (4-1/2)	11 (4-1/2)	Two separate scrapes, one shown from each camera
5	11 (4-1/2)	11 (4-1/2)	Single scrape photographed by both cameras
6	13 (5)	13 (5)	Two separate scrapes, one shown from each camera
7	10 (4)	10 (4)	Two separate scrapes, one shown from each camera
8	No photography	11 (4-1/2)	Two separate scrapes shown from one camera
9	No photography	No scrapes	Penetrator paint undamaged
10	11 (4-1/2)	11 (4-1/2)	Two separate scrapes, one shown from each camera
	42 (16-1/2)	No scrapes	Single scrape shown only by one camera
	57 (22-1/2)	No scrapes	Single scrape shown only by one camera
11	11 (4-1/2)	11 (4-1/2)	Two separate scrapes, one shown from each camera
	42 (16-1/2)	42 (16-1/2)	Two separate scrapes, one shown from each camera
	57 (22-1/2)	57 (22-1/2)	Two separate scrapes, one shown from each camera
12	10 (4)	11 (4-1/2)	Two separate scrapes, one shown from each camera
	41 (16)	No scrapes	Single scrape shown only by one camera
	51 (20)	No scrapes	Single scrape shown only by one camera
13	13 (5)	13 (5)	Two separate scrapes, one shown from each camera

<sup>a</sup>Scrape marks are defined as locations where the white paint on the surface of the penetrator has been abraded away exposing a black undercoat, zinc chromate primer, or bare metal. Scrape areas typically cover several square inches.

<sup>b</sup>Measured to within  $\pm 1/4$  inch.

TABLE IV.- STATUS OF HIGH-SPEED MOTION PICTURE FILM

Shot no.	Camera, station	Description of image	Quality rating (a)	Timing original, Hz
1	Hycam, 1	See 5 stripes, all are blurred and 1 cm (1/2 in.) thick	E	Incomplete IRIG A
	Fastax, 2	See 7 stripes, last one is very faint	F	No IRIG A
2	Hycam, 1	See 7 stripes	F	Incomplete IRIG A
	Fastax, 2	See 7 stripes	F	No IRIG A
3	Fastax, 2	See 7 stripes, faint	F	No IRIG A
	Hycam, 1	See 7 stripes	F	Incomplete IRIG A
4	Hycam, 1	See 7 stripes	A	10 000
	Fastax, 2	See 7 stripes, 3 are very faint	B	100 10 000
5	Fastax, 2	See 7 stripes, all are blurred and 1 cm (1/2 in.) thick, last 2 very faint	B	1 000 10 000
	Hycam, 1	See 7 stripes, last 2 very faint	B	1 000 10 000
6	Hycam, 1	See 7 stripes, all very faint	B	1 000 10 000
	Fastax, 2	See 7 stripes for 50 percent of field of view only	B	100 10 000
7	Hycam, 1	See 7 stripes, all very faint	B	1 000 10 000
	Fastax, 2	See 5 stripes, all blurred and <u>very</u> faint	E	100 10 000
8	Fastax, 2	See penetrator nose only	E	1 000 10 000
	Hycam, 1	No film	G	1 000 --
9	Fastax, 2	See penetrator nose only	E	10 000 1 000
	Hycam, 1	No film	G	-- --
10	Fastax, 2	See 7 stripes, blurred and very faint	C	1 000
	Hycam, 1	See 7 stripes, sharp image	D	100
11	Hycam, 1	See 7 stripes, sharp image	D	100
	Fastax, 2	See 7 stripes	C	1 000
12	Hycam, 1	See 7 stripes, sharp image	A	10 000
	Fastax, 2	See 5 stripes, only at edge of penetrator	E	100 1 000
13	Hycam, 1	See 7 stripes, sharp image	A	10 000
	Fastax, 2	See 7 stripes, very faint only at edge of penetrator	C	100 1 000

<sup>a</sup>Quality rating assigned after four successive film processing improvements. Key to quality rating of films after fourth processing: A, see seven stripes sharp enough to measure, has 10 000-hertz timing marks (three films); B, see seven stripes but some may be too faint to measure, has 10 000-hertz timing marks (six films); C, see seven stripes but some may be too faint to measure, has 1000-hertz timing marks (three films); D, see seven stripes sharp enough to measure, has only 100-hertz timing marks (two films); E, see one or more stripes but some (or all) may be too faint to measure, has 10 000-, 1000-, or 100-hertz timing marks (five films); F, see seven stripes which may be sharp or faint but has no timing marks (five films); and G, cannot see penetrator (two shots).

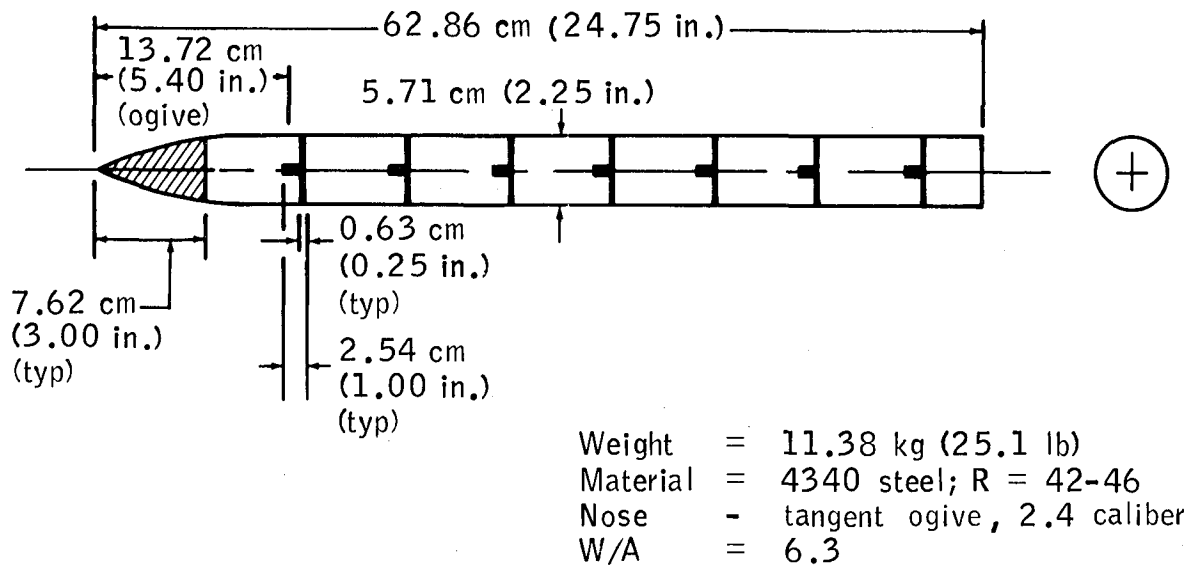


Figure 1.- Mars penetrator (0.63 scale) configuration fired in tests at Tonopah, Nevada, in April 1979.

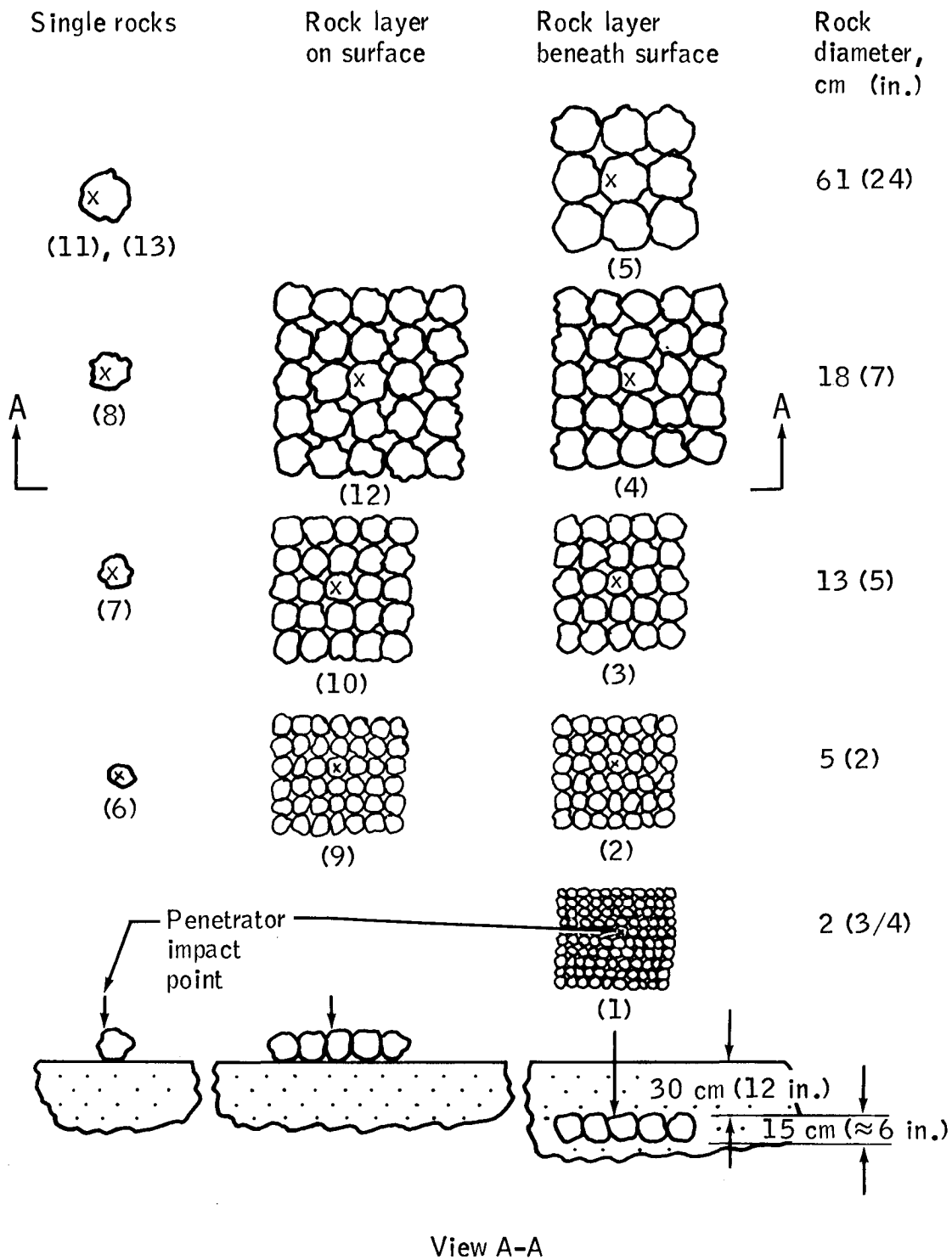


Figure 2.- Layout of test site. The penetrator impact points are located at one-half the radius of the rock. Test numbers are shown beneath each target arrangement.



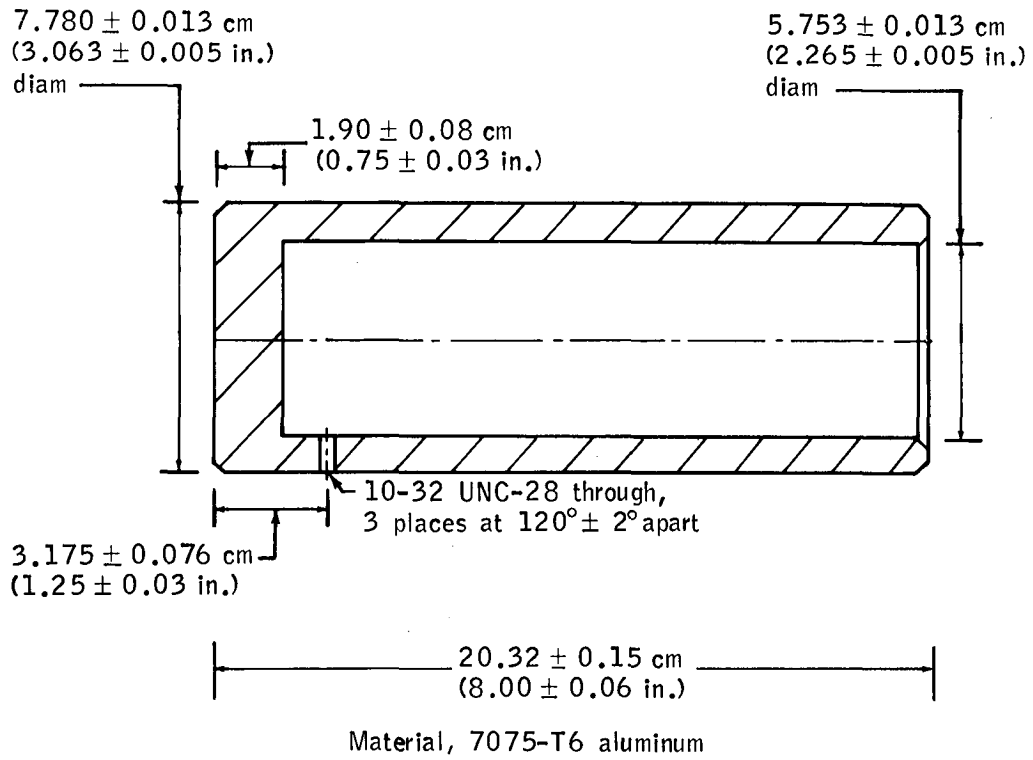


Figure 3.- Sabot used to adapt penetrator to 7.6-centimeter (3 inch) air gun.



Figure 4.- Penetrator and sabot assembled and mounted in breech of air gun.

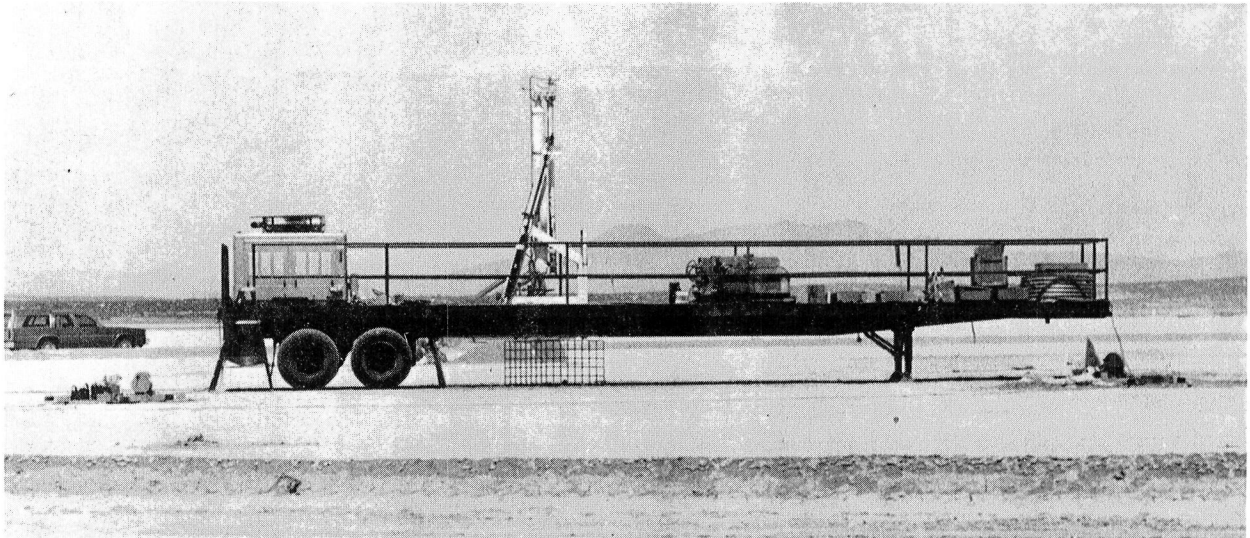


Figure 5.- Air gun shown in vertical position (orientation from which measurements were made) and grid frame located beneath trailer before test 6. Camera pallets are located on the ground near the front and rear of the trailer.

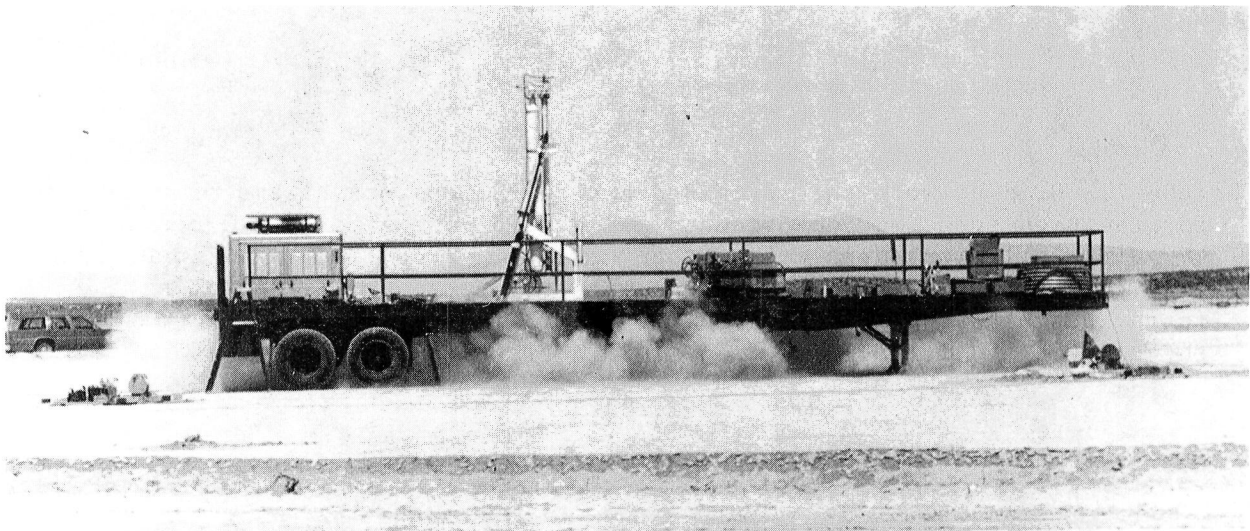


Figure 6.- Penetrator being fired by air gun (test 6). The blast of air which replaces the penetrator produces the cloud of dust obscuring the grid and the target.

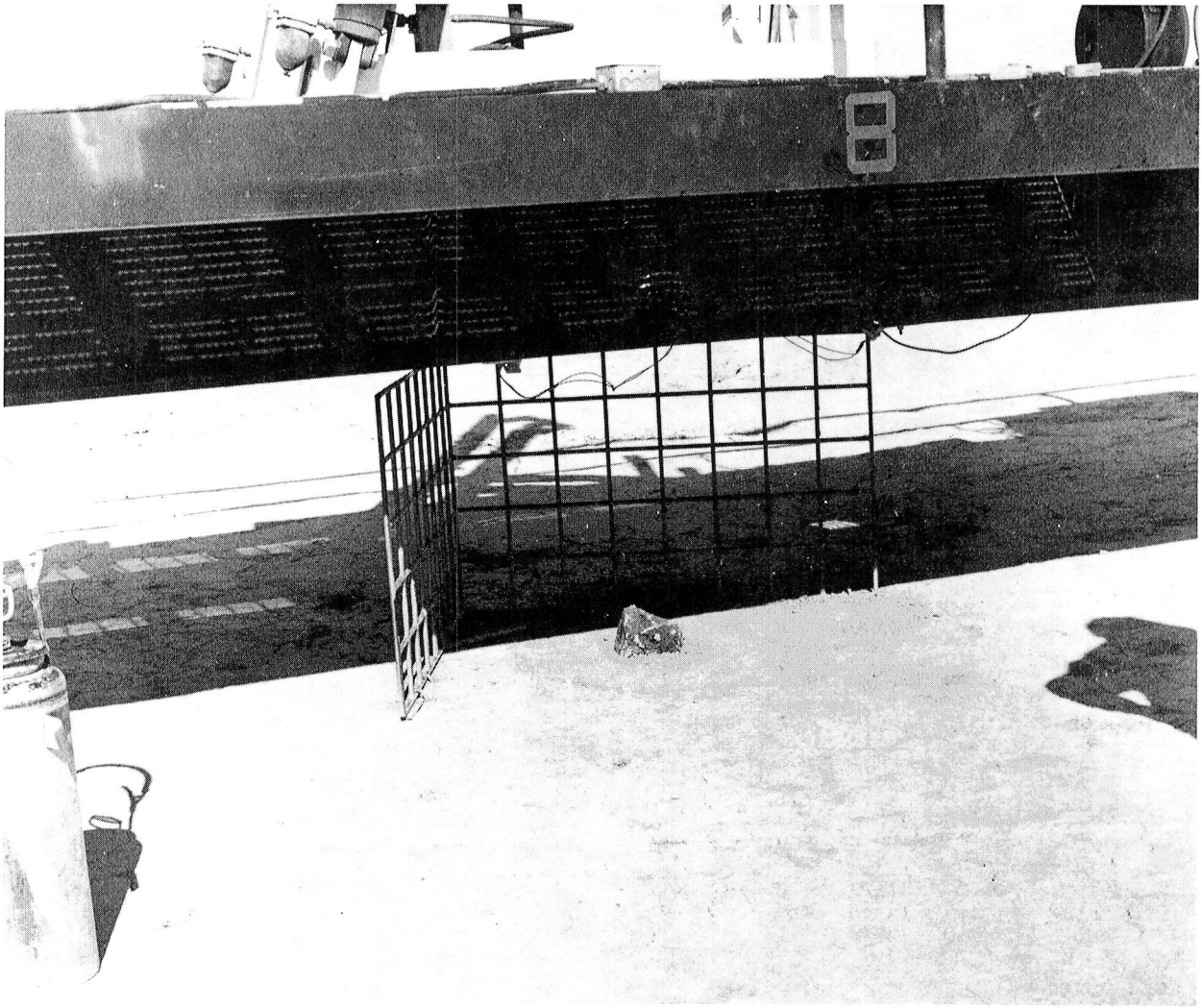


Figure 7.- Grid network that provided a three-dimensional frame of reference for the high-speed motion pictures. The grid consisted of 1.3-centimeter (0.5 inch) aluminum bars welded together at 15.2-centimeter (6 inch) intervals. The grid was staked to the ground to prevent movement during the tests, but airblast-produced vibration occasionally blurred the image of the grid in the films.

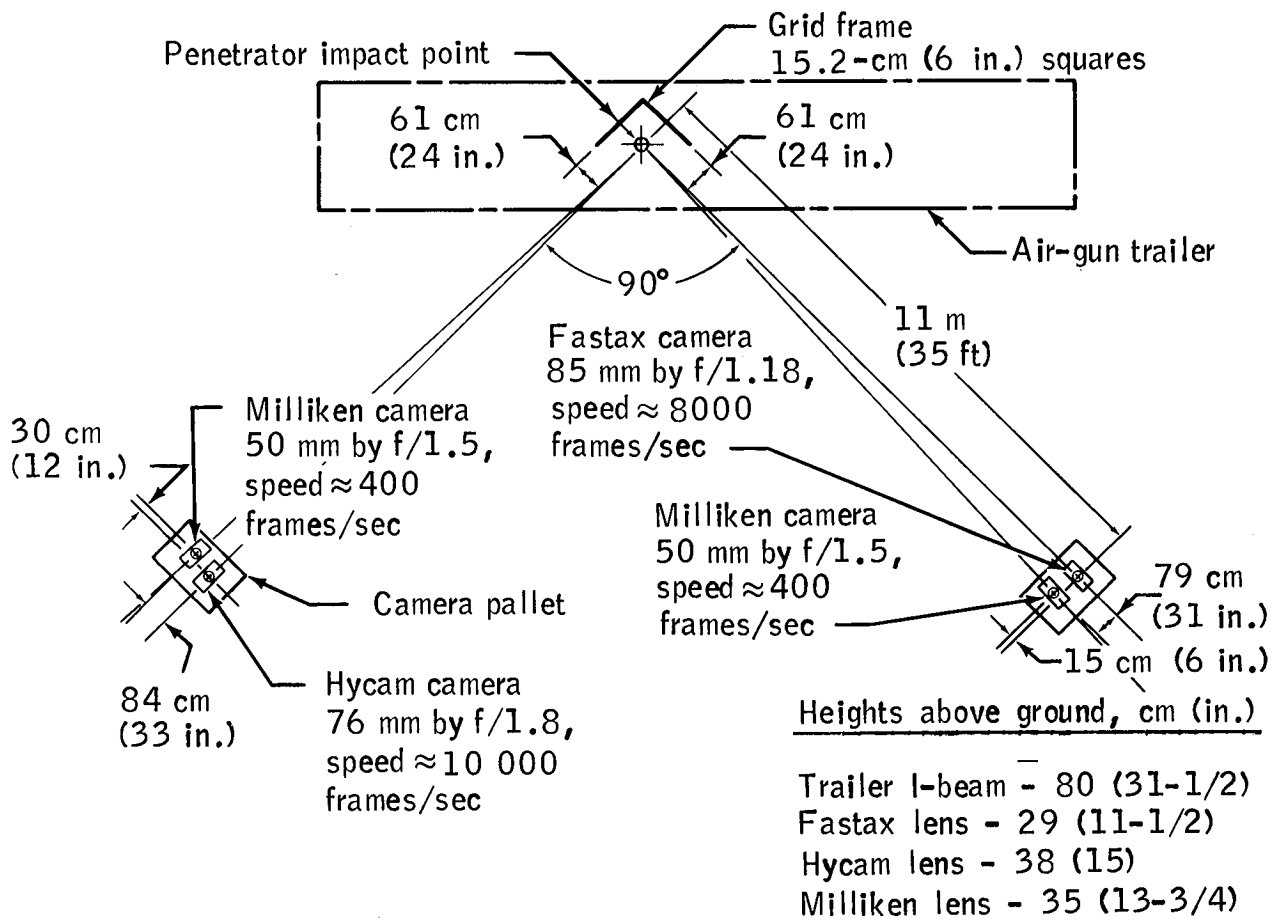


Figure 8.- Layout of motion picture cameras, grid frame, and penetrator impact point.

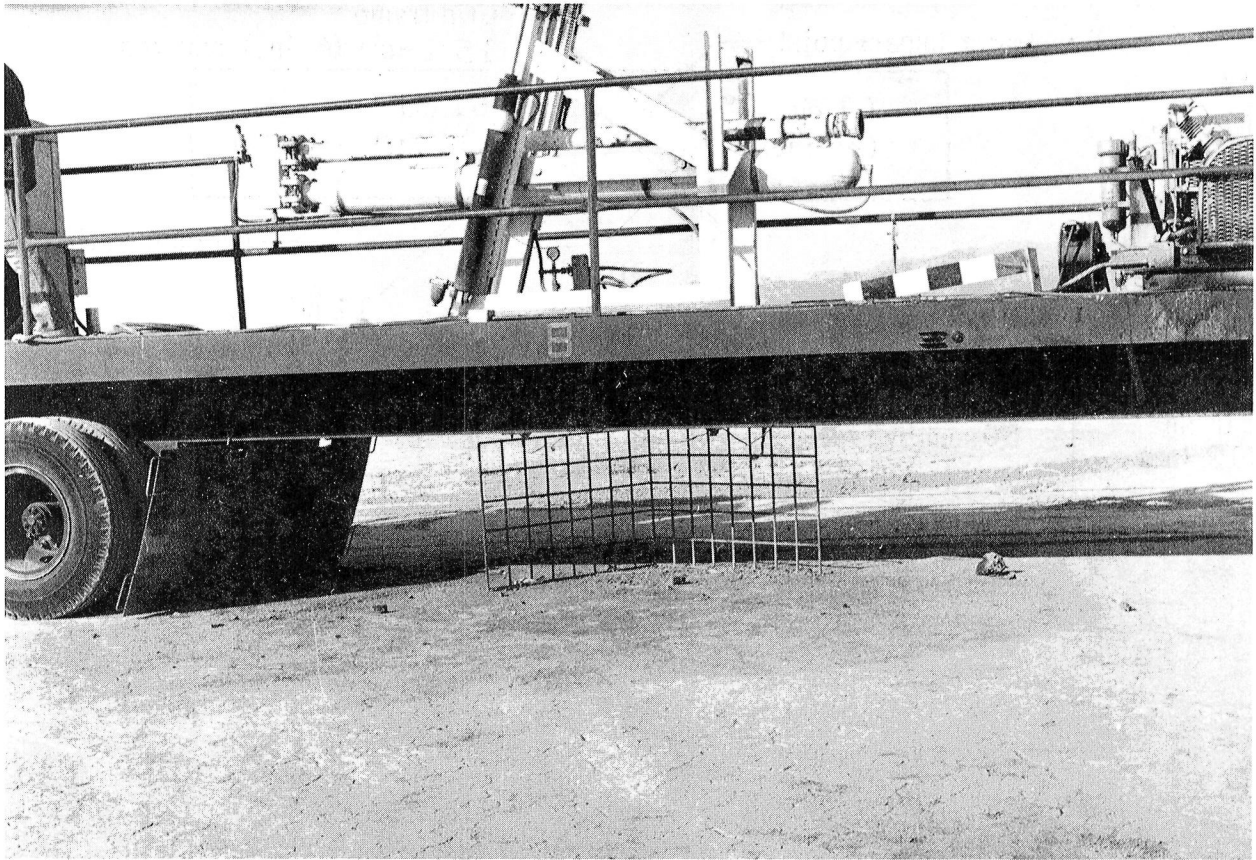


Figure 9.- Cratered area after penetrator passed through the 13-centimeter (5 inch) diameter rock shown in figure 7. The penetrator stopped approximately 4 meters (12 feet) beneath the surface after impact. Several broken fragments of the original rock are near the grid.

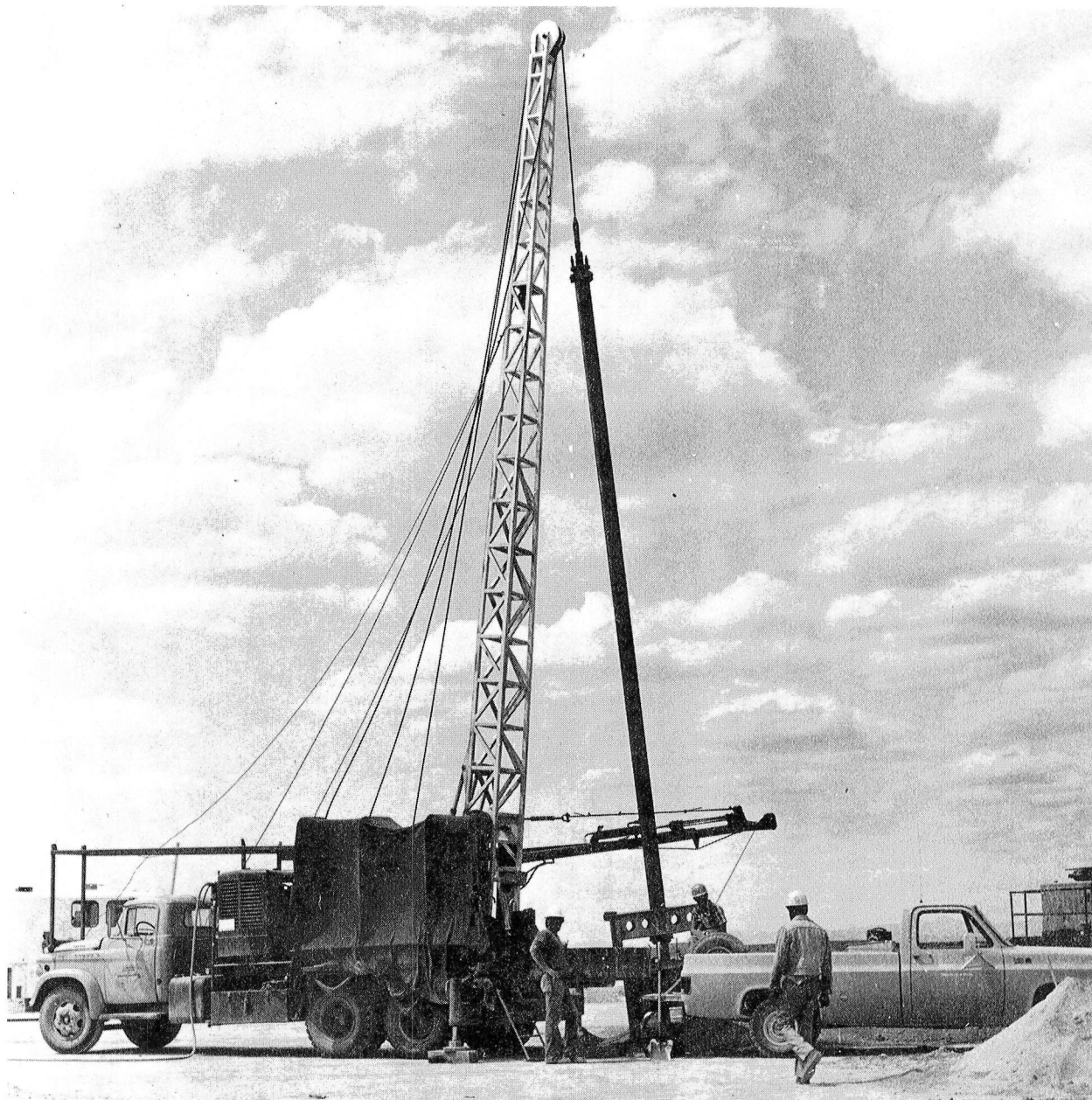


Figure 10.- A 1.2-meter (4 foot) diameter hole was drilled with a bucket auger adjacent to the hole made by the penetrator.



Figure 11.- One side of the hole was removed to expose a complete cross section of the hole made by the penetrator.



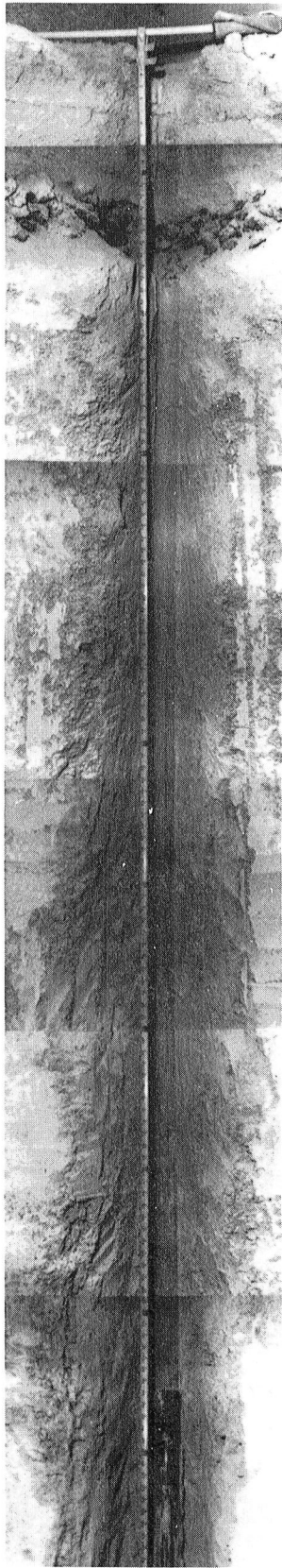
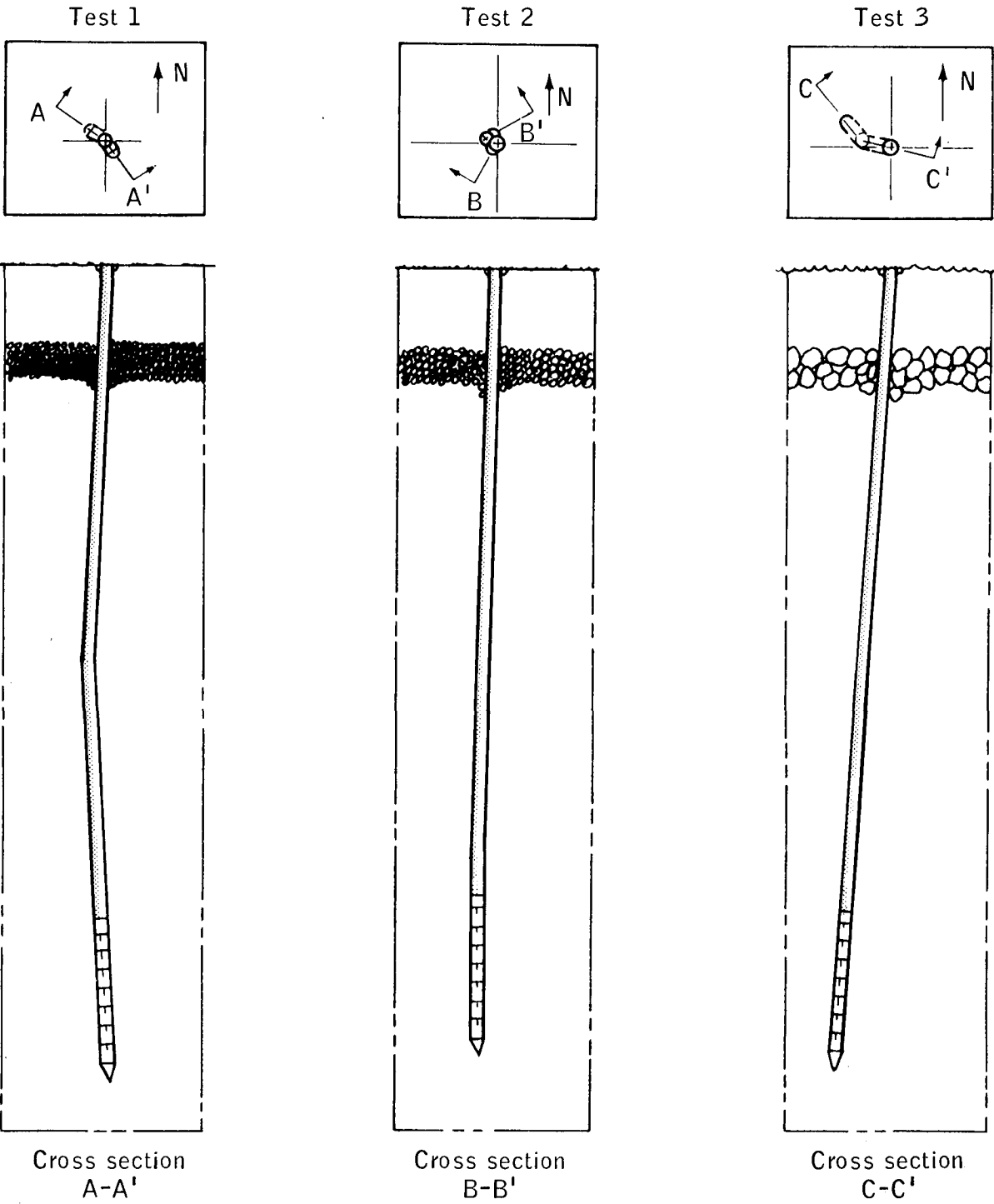
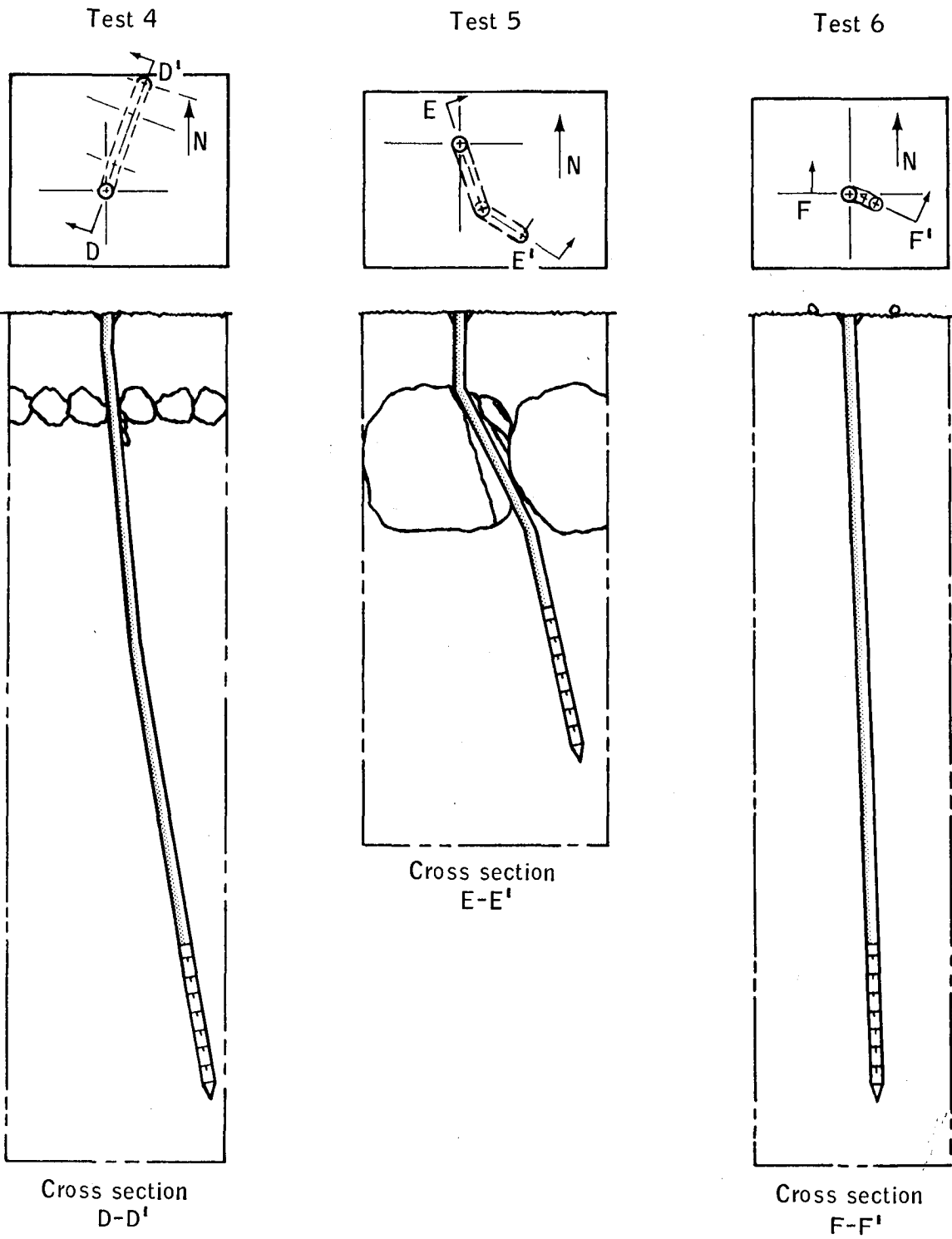


Figure 12.- Cross section of the hole made by the penetrator in test 2. The distance from the surface of the ground to the nose of the penetrator is 323 centimeters (127 inches). The penetrator had a final orientation of  $89^{\circ}20'$  from the horizontal along a bearing of  $60^{\circ}$ . A change in direction occurred just after the penetrator passed through the 5-centimeter (2 inch) diameter rocks.



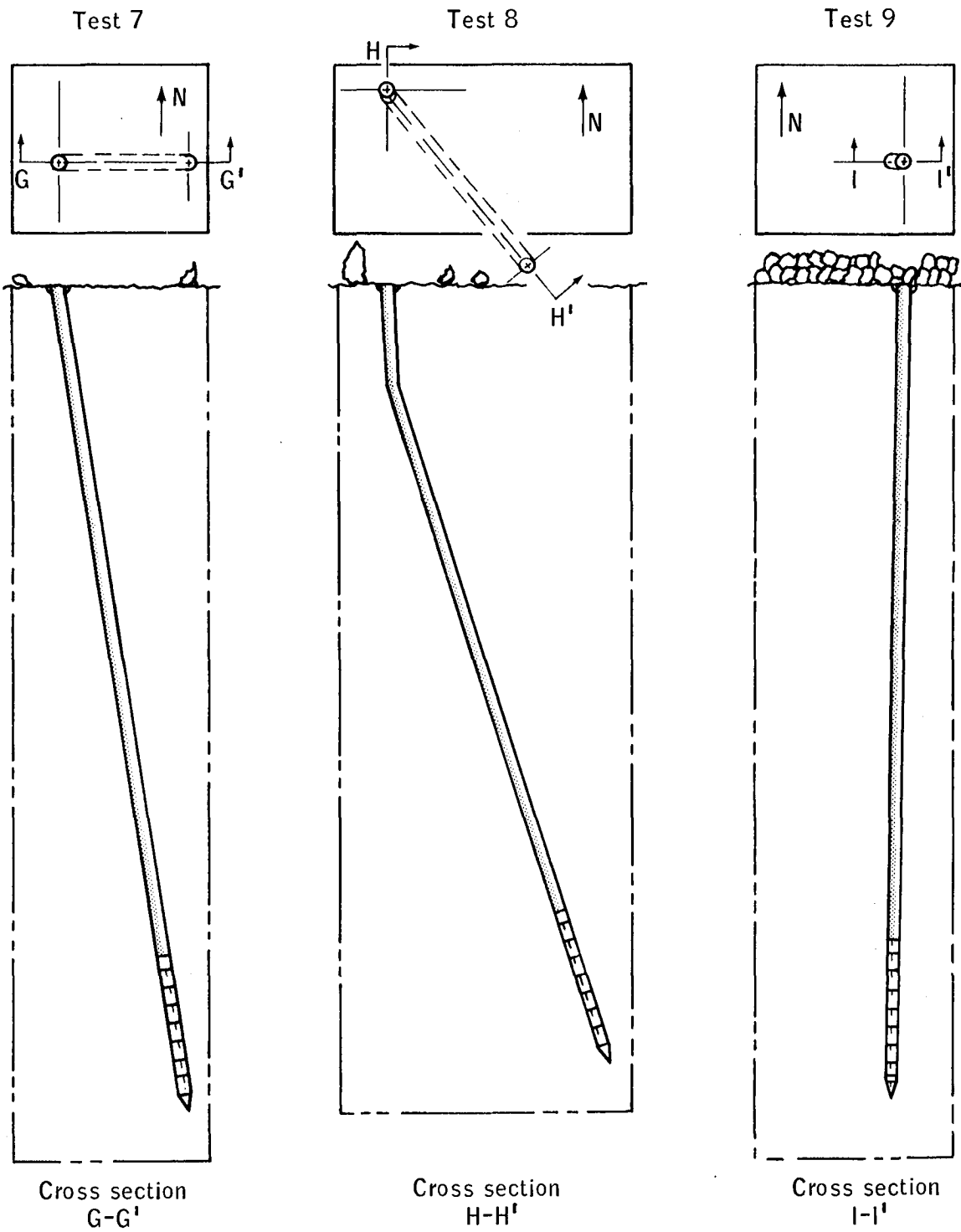
(a) Tests 1 to 3.

Figure 13.- Cross sections of the hole after each penetrator test.



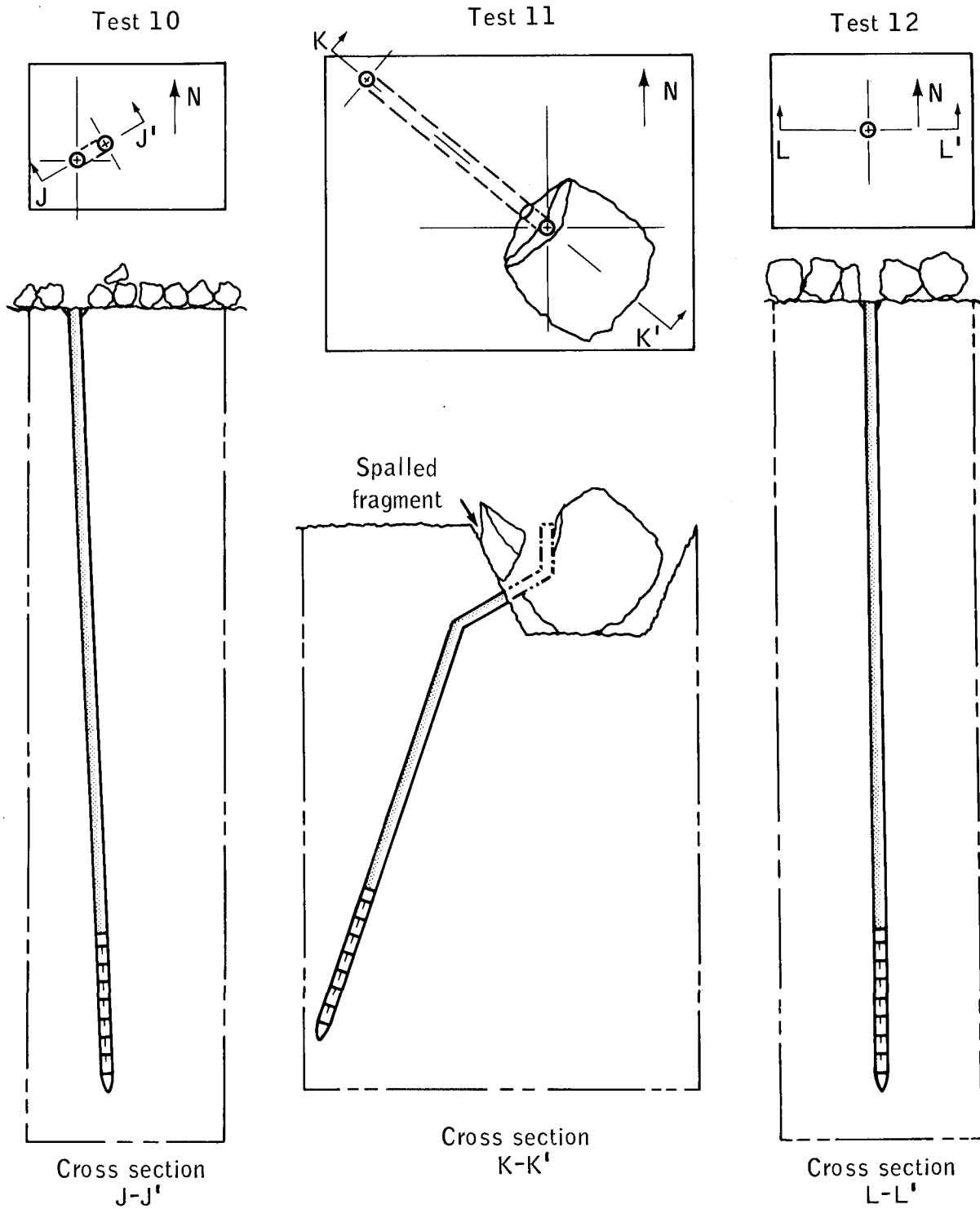
(b) Tests 4 to 6.

Figure 13.- Continued.



(c) Tests 7 to 9.

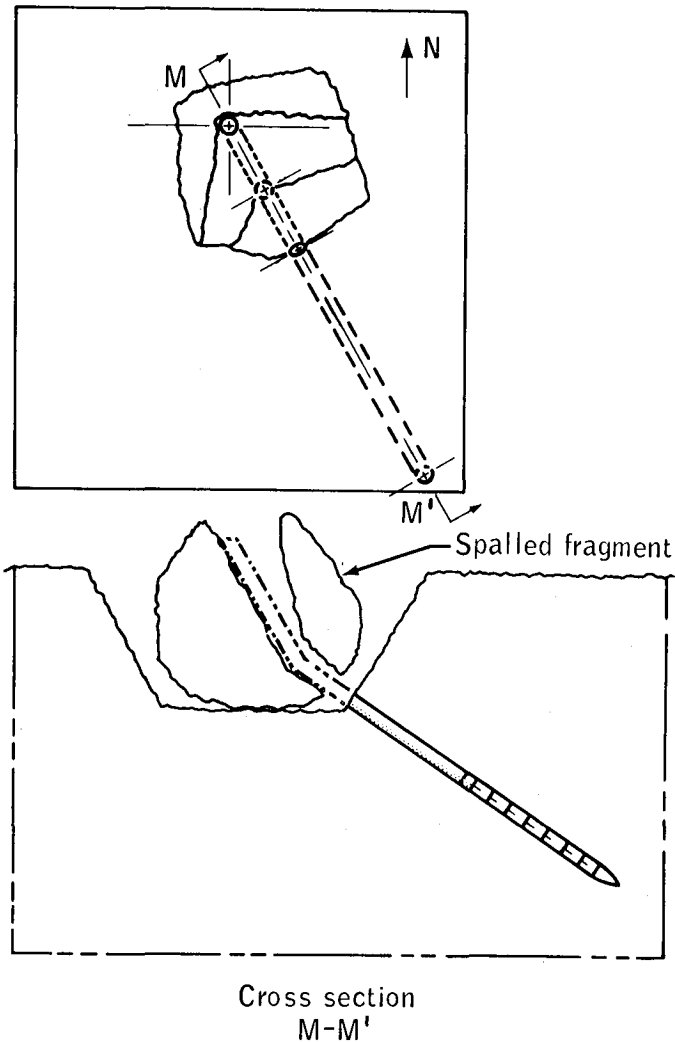
Figure 13.- Continued.



(d) Tests 10 to 12.

Figure 13.- Continued.

Test 13

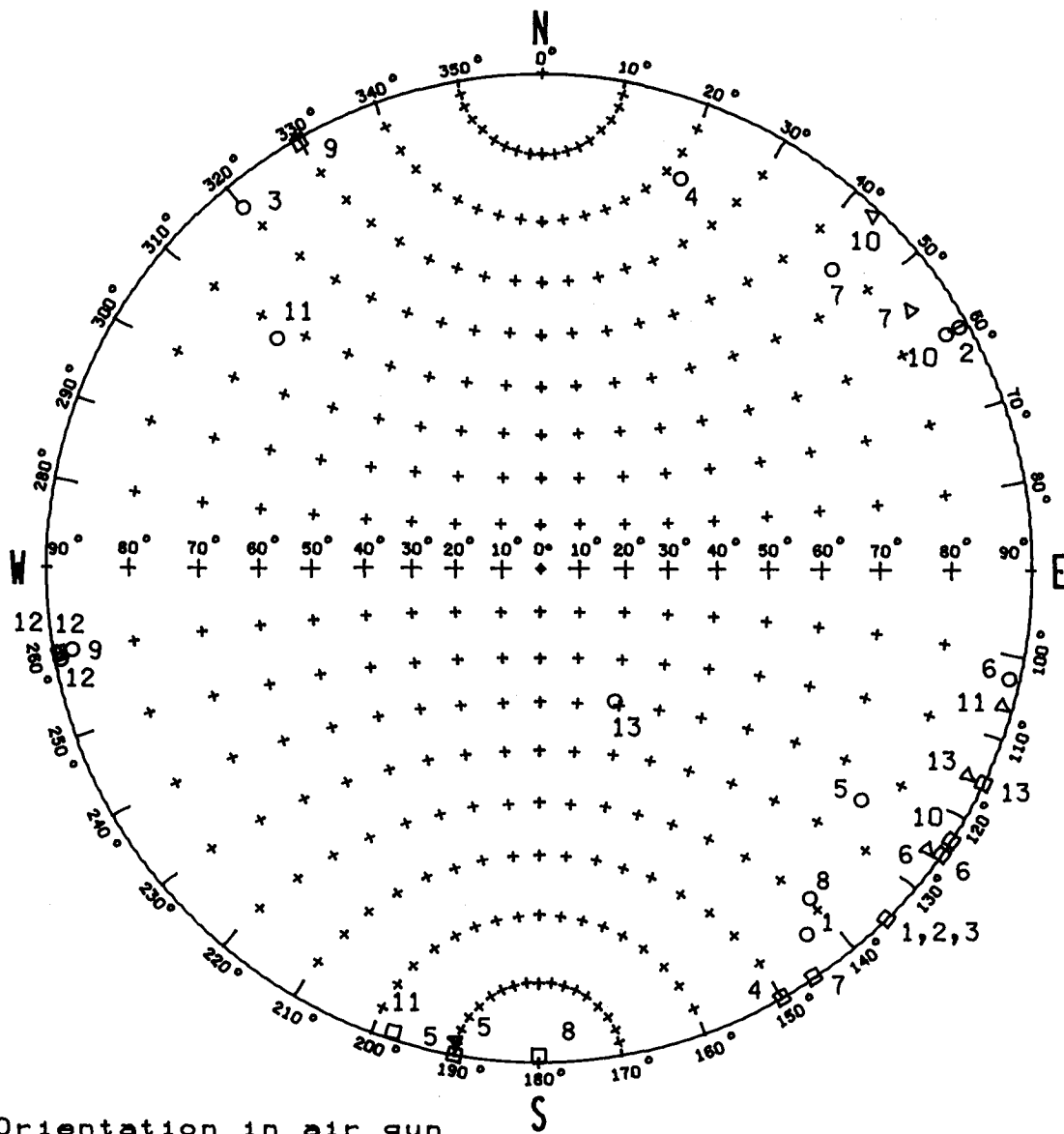


NOTES

1. These diagrams have been reconstructed from field measurements and are intended to show only major changes in penetrator direction. The diagrams only approximate the actual penetrator movement.
2. The diagrams only approximate the location and shape of the rocks the penetrator encountered. Rock boundaries have been omitted for clarity in plan views of tests 1 to 10 and 12.

(e) Test 13.

Figure 13.- Concluded.



- Orientation in air gun
- △ Free-flight orientation
- Final orientation

Figure 14.- A cyclographic projection showing penetrator orientations for each test. Three points were plotted for tests 5, 6, 7, 10, 11, 12, and 13: orientation in the air gun (data from table I), orientation during free flight (data from high-speed motion pictures), and final orientation (data from table II). Two points were plotted for all other tests: orientation in the air gun and final orientation. The bearing for each point is read on the outside perimeter as a compass direction. The dip angle is read along a radius from the origin to either E or W using the graduated 10° increments from 0° to 90°. The procedure used to locate these points is described in reference 6.

1. Report No. NASA TM-58222		2. Government Accession No.		3. Recipient's Catalog No.	
4. Title and Subtitle PRELIMINARY RESULTS OF PENETRATOR FIELD TEST PROGRAM--TONOPAH, NEVADA, APRIL 16-28, 1979				5. Report Date October 1979	
				6. Performing Organization Code JSC-16221	
7. Author(s) Maxwell B. Blanchard, Uel Clanton, and Victor Rhoder, JSC, Mischelle Dalbey, LPI, and James P. Murphy, ARC				8. Performing Organization Report No.	
				10. Work Unit No. 152-85-00-00-72	
9. Performing Organization Name and Address  Lyndon B. Johnson Space Center Houston, Texas 77058				11. Contract or Grant No.	
				13. Type of Report and Period Covered  Technical Memorandum	
12. Sponsoring Agency Name and Address  National Aeronautics and Space Administration Washington, D.C. 20546				14. Sponsoring Agency Code	
15. Supplementary Notes  Mischelle Dalbey was a summer intern at the Lunar and Planetary Institute.					
16. Abstract  Thirteen subscale (0.63 scale) penetrators impacted various sizes of volcanic rocks resting on and within compacted playa sediments at Tonopah Test Range, Nevada, during April 1979. All penetrators were identical in size, shape, weight, and impact velocity. Although minor variations in impact angle were documented, the <u>final</u> orientation of the buried penetrators was primarily a consequence of the size, shape, and depth of the rocks encountered during impact. In situ measurements of impacted penetrators revealed that surface and buried layers of rocks having diameters up to 3 times the penetrator diameter caused only small (<10°) angles of deflection. Only large single rocks greater than 10 times the penetrator diameter caused deflections appreciably greater than 10°. The large deflection angles followed by the penetrator were strongly influenced by fracture planes that developed in the rock as it broke apart. No catastrophic failure of the penetrator occurred during these tests. A cross section of the path of each penetrator through the ground is shown together with details on orientation before, during, and after the tests. Comparisons are made with results of previous subscale penetrator tests, and conclusions are drawn with respect to full-scale Mars penetrator performance.					
17. Key Words (Suggested by Author(s))  Penetrators Fracture mechanics High-speed cameras Mars exploration Planetary missions			18. Distribution Statement  STAR Subject Category: 91 (Lunar and Planetary Exploration)		
19. Security Classif. (of this report) Unclassified		20. Security Classif. (of this page) Unclassified		21. No. of Pages 36	22. Price* \$4.00

\*For sale by the National Technical Information Service, Springfield, Virginia 22161





1000